Journal of Sol-Gel Science and Technology (2024) 111:61–72
https://doi.org/10.1007/s10971-024-06429-2

ORIGINAL PAPER

Preparation of high transparent hydrophobic glass surface and its self-cleaning property

Jiefang Li[1] · Que Kong[2] · Dan Zhang[1] · Zhiguang Li[1,3]

Received: 21 March 2024 / Accepted: 21 May 2024 / Published online: 3 June 2024

Abstract

Transparent hydrophobic glass materials had played an important role in our daily life, but some problems such as complex or expensive manufacturing processes, poor wear resistance and opacity limited its applications. In this paper, a composite silica sol composed of modified SiO_2 nanoparticles and transparent special water-based silicone resin was prepared. An organic-inorganic hybrid coating was formed on the glass surface by a simple spraying method to produce a hydrophobic surface with high transparency and durability. Perfluorinated polyether (PFPE) chains with lower surface energy were introduced into the silica sol prepared above. The composite coatings had both the low surface energy of fluorine-containing substances and the rough structure. The surface topography, static water contact angle, self-cleaning performance, anti-fouling performance, wear resistance, adhesion performance, acid and alkali resistances of the coating were tested. The results showed that the maximum water contact angle of the prepared transparent hydrophobic glass can reach 140°. The coating had good adhesion performance, wear resistance, self-cleaning and acid resistant, but poor alkaline resistance.

Graphical Abstract

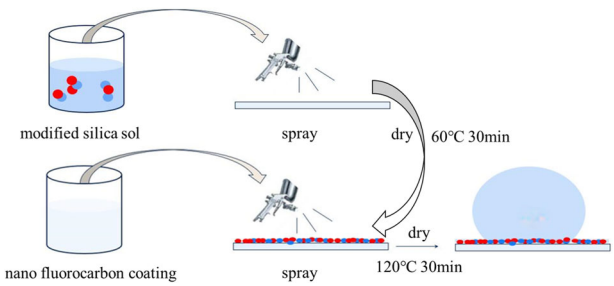

Keywords Transparent and wear-resistant · Hydrophobic · Sol-gel method · SiO_2 modification · Perfluorinated polyether chain

✉ Dan Zhang
zhangdan@jiangnan.edu.cn

✉ Zhiguang Li
lizg@jiangnan.edu.cn

[1] Key Laboratory of Eco-textiles of Ministry of Education, College of Textile Science and Engineering, Jiangnan University, Wuxi 214122, China

[2] College of Textile and Garment, Jiangsu Advanced Textile Engineering Technology Center, Jiangsu College of Engineering and Technology, Nantong 226007, China

[3] Hubei Key Laboratory of Biomass Fibers & Eco-Dyeing & Finishing, Wuhan Textile University, Wuhan 430200, China

Highlights

- Wear-resistant self-cleaning silicon sol coating was developed.
- Perfluorinated polyether (PFPE) chains improved the hydrophobicity of the surfaces.
- The effect of KH550 and KH560 with different volume ratios on the coating properties was investigated.
- Hydrophobic coating was developed on glass substrates by spray-coating.

1 Introduction

In daily life, glass fiber is a widely used inorganic non-metallic material, its main components include silicate, silica and other substances. High transmission hydrophobic glass allows for many potential applications, including anti-frost [1–3], self-cleaning materials [4, 5], anti-icing materials [6, 7], anti-corrosion [8–10], sensors [11], oil/water separation [12, 13], fabrics [14]. However, in practical application scenarios, because the glass is generally exposed to the air, its surface is polluted by dust particles, which will significantly reduce the transmission of light. Especially in the photovoltaic application scenario, the pollution of the glass surface of solar panels is one of the main problems affecting the performance of photovoltaic modules [15]. Sulaiman et al. had found that dust particles on the glass surface of the panel will reduce its efficiency by 85% [16]. In order to solve this problem, regular artificial cleaning of the glass surface needs to consume lots of financial and material resources. Therefore, the development of self-cleaning glass with hydrophobic property has become a research hotspot.

In 1997, through the observation of the surface morphology of lotus leaves, low surface energy substances and the micro-nano level rough structure were the key factors to make the solid surface have hydrophobic properties [17]. Since then, the preparation method of superhydrophobic surface has been widely studied. However, there are few researches on transparent hydrophobic coating. Because from the point of view of surface roughness, hydrophobicity and transparency are competing properties [18]. According to Akria et al., controlling the rough structure to less than 100 nm was conducive to the simultaneous realization of both transparent and hydrophobic properties [19].

Numerous techniques have been utilized to prepare superhydrophobic coatings, including electrochemical method [20], dip coating method [21, 22], etching method, spray method [23, 24], self-assembly method [25] and sol-gel method [26]. Sol-gel method is a common method for preparing organic-inorganic hybrid materials. The preparation method is to dehydrate and condense esters or metal salts as precursors to form a gel with a three-dimensional network structure. The sol with different surface structures can be obtained by adjusting the composition of the precursors and the sol-gel preparation process. Bake [27] et al. adopted the sol-gel method, using the appropriate molar ratio of methyl trimethoxy-silane (MTMS) and γ-(2, 3-epoxy-propoxy-propyl) propyl trimethoxy-silane (KH560) silanized adhesive as the primer, and then 1H, 1H, 2H, 2H-perfluorooctane-trichlorosilane (PFOTS) modified SiO_2 nanoparticles sprayed on the primer obtained a strong and super-hydrophobic coating with a transmittance of 6% higher than that of bare glass, mainly due to the reduction of surface reflectivity caused by the rearrangement of SiO_2 nanoparticles. Zhang et al. hydrolyzed KH-560 and added polyethylene glycol as a pore-forming agent to prepare a nanoporous structural layer solution. The glass coated with the structural layer solution successfully formed a porous cross-linked network structure after calcination at high temperature, and then embedded modified hydrophobic sol-gel SiO_2 nanoparticles in the porous network structure to obtain a permeability of up to 97%. Superhydrophobic surface with refractive index reduced to 1.3471. In addition to the above methods, there are many methods to construct hydrophobic coatings on the glass surface, such as electrostatic spinning [28, 29], chemical vapor deposition [30], phase separation [31]. Each method has its own advantages and disadvantages in terms of preparation procedure, preparation scale, process cost, film performance, etc. The selection of specific methods needs to be determined according to the actual requirements and the environment used. However, no matter what kind of use environment, the mechanical stability and environmental stability of the structure and performance of the surface have certain requirements.

For inorganic materials such as glass, in order to prepare superhydrophobic surfaces, the current methods often use substances containing elements such as carbon and fluorine to combine with them to form organic-inorganic hybrid coatings with micro-nano rough structures. However, after such micro and nano structures are constructed on the glass surface, the mechanical stability of the transparent hydrophobic coating is often affected due to it is usually in thermodynamic metastable state. At the same time, there are a lot of pores and micro-cracks on the surface of the glass, which will lead to the deterioration of its wear resistance. Therefore, the functional modification of glass surface can effectively improve its self-cleaning ability and the wear resistance of the coating without affecting its light transmittance, which has become an important direction for the functional modification of glass surface [32].

In this paper, ethyl orthosilicate (TEOS) was used as a precursor to prepare SiO_2 sol under the action of alkali catalysis. Then the prepared silica sol was functionalized with silane coupling agent. The water-based silicone resin

was added to obtain the modified silica sol with good dispersion and stability, which was sprayed on the glass substrate surface. A rough structure with organic/inorganic nanocomposite was constructed. After spraying nano fluorocarbon polymer, which was equivalent to using low surface energy material perfluoropolyether polymer for surface modification, spraying on the glass to obtain a chemically bonded composite coating. Finally, the X-ray energy spectrometer (EDS) analysis, scanning electron microscopy (SEM) and fourier transform infrared spectroscopy (FTIR) of composite coating materials were carried out. In addition, a series of performance tests were conducted to evaluate coating properties and study the relationship between material structure and properties, including self-cleaning performance test, anti-fouling performance test, wear resistance test, adhesion test, acid and alkali resistance tests.

2 Experiment

2.1 Materials

25 mm × 60 mm glass slides were purchased from Shanghai Xingtai Industrial Glass Co., Ltd. Ethyl orthosilicate (TEOS) was purchased from Shanghai Chemical Reagent procurement and supply of Wulian Chemical Plant. The glass slides were ultrasonic cleaned with acetone and anhydrous ethanol respectively for 20 min, the dust and oil on the glass substrate were removed. Then the slides were dried in the blast drying oven at 80 °C for use. γ-aminopropyl triethoxysilane (KH550) was purchased from Beijing Innokai Technology Co., LTD. RS-9711 water-based nano silicone resin was purchased from Zhongshan Kobang Chemical Material Technology Co., LTD. Acetic acid, anhydrous ethanol, hydrochloric acid (HCl), sodium hydroxide(NaOH), aqueous ammonia and γ-(2,3-epoxypropoxy)propytrimethoxysilane (KH560) were purchased from Sinopharm Chemical reagent Co., Ltd. Quartz sand was purchased from Shanghai McBiochemical Technology Co., Ltd. QX-18 fluorocarbon nanocoating was purchased from Nanjing Quanxi Chemical Co., Ltd.

2.2 Preparation of SiO_2 sol

3 mL of 30% ammonia and 20 mL of anhydrous ethanol were added into a 50 mL beaker. The solution was sealed and stirred for 30 min at room temperature. Then 25 mL anhydrous ethanol and 3 mL ethyl orthosilicate were added into another 50 mL beaker, sealed and stirred for 30 min at room temperature. Under the condition of intense stirring, the solution in the two beakers was added to the three-neck flask, and the nano-SiO_2 sol was obtained by sealing and stirring under the condition of 50 °C water bath for 1 h. The prepared silica sol was poured into the beaker and stirred for 12 h to make the ammonia in the sol volatilize and ensure the stability of the SiO_2 sol.

2.3 Silane coupling agent modified SiO_2 sol

50 mL anhydrous ethanol was added into the prepared silica sol, adjusted the solid content to 2–3%. 10 mL deionized water were added to 1 mL silica sol and the pH was adjusted at 3~4 by adding acetic acid. KH560 and KH550 were added to the solution, and the volume ratio of the KH560 and KH550 was 1:1. Moreover, after magnetic stirring at room temperature for 30 min, 0.2 mL of RS-9711 water-based nano silicone resin were added to the solution under the condition of intense stirring, and the silane coupling agent modified SiO_2 sol was obtained by continuing to seal and stir for 4 h.

2.4 Preparation of transparent hydrophobic wear-resistant glass surface

A spray was used to continuously spray the composite silica sol onto the substrate and form a thin liquid film. The coated substrate was dried in an oven at 60 °C for 30 min. After being placed at room temperature, the QX-18 fluorocarbon nano coating was sprayed onto the glass surface coated with composite silica sol (0.1 mL/cm^2), and finally dried in the oven at 120 °C for 30 min. At high temperature, silanization graft reaction was occurred between the PFPE molecular chain and the silicon hydroxyl group, thus the chemically bonded transparent wear-resistant hydrophobic composite coating was obtained (Fig. 1).

2.5 Preparation mechanism of composite coating

2.5.1 Mechanism analysis of SiO_2 modification by silane coupling agent

SiO_2 sol was prepared with TEOS as precursor and ammonia as catalyst. Silane coupling agents KH550 and

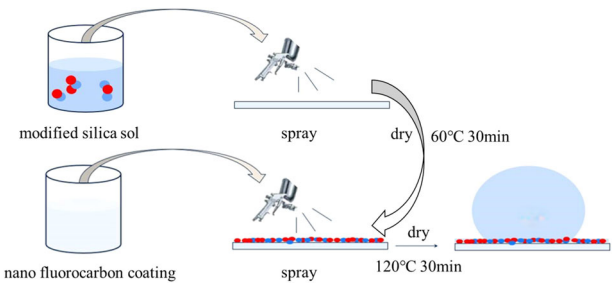

Fig. 1 Preparation process and hydrophobic properties of transparent wear-resistant hydrophobic glass

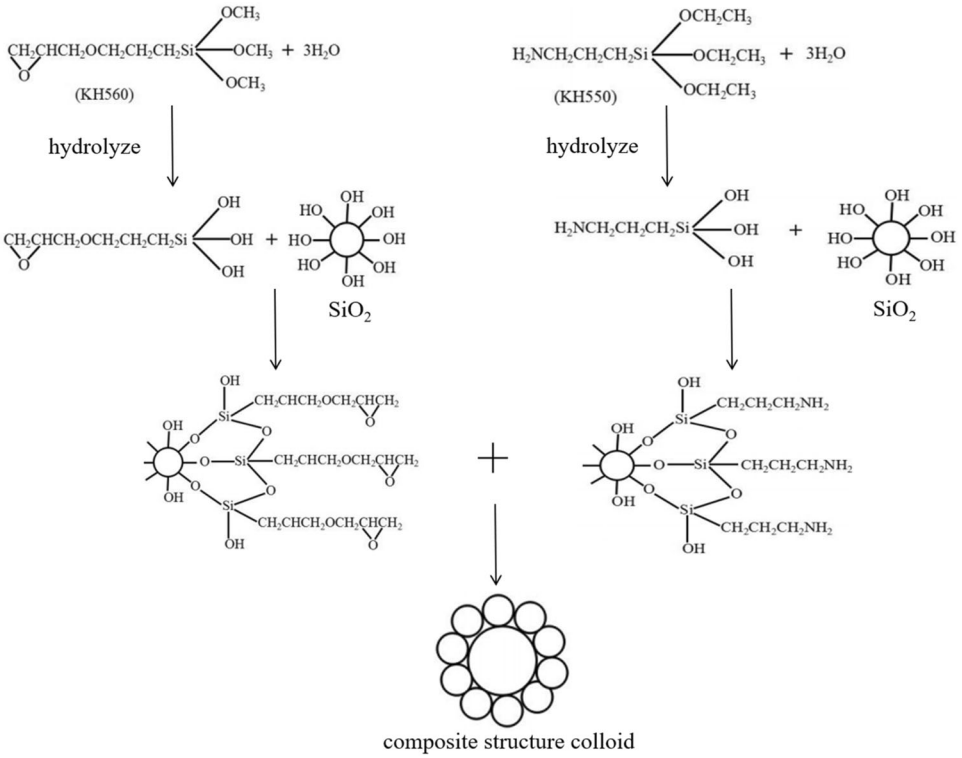

Fig. 2 Modification principle of silane coupling agent

KH560 with different functional groups on the surface were used to modify the silica sol. The two silane coupling agents reacted with SiO_2 colloidal particles respectively to obtain a composite structure colloid with two kinds of colloidal particles, and a rough surface with binary layers in the microstructure was obtained. The corresponding reaction equations of organic-inorganic hybrid silane coupling agent were shown in Fig. 2.

2.5.2 Grafting mechanism analysis of perfluorinated polyether chain and modified SiO_2 sol

Firstly, the hydroxyl groups of the modified silica sol underwent grafting reaction with the hydroxyl groups on the surface of the glass slide. The hydroxyl group on the surface of the perfluoropolyther polymer (PFPE) in the nano fluorocarbon coating underwent polycondensation with the unreacted hydroxyl group in the modified SiO_2 microspheres during heating, forming stable Si-O-Si bonds. By chemically bonding the PFPE chain with the modified silica sol, a composite coating with better hydrophobic property was obtained.

2.6 Characterization

The functional groups of coatings were characterized by FTIR spectroscopy (Nicolet iS20, Thermo Scientific, USA). The micromorphology of the hydrophobic coating was observed on a scanning electron microscope [33]. The elemental analysis test of the transparent hydrophobic coating was performed using an EDS in combination with the scanning electron microscope (SU1510, Hitachi, Japan). The transmittance of the composite coating was tested using Perkin Elmer's Lambda 950 UV visible near-infrared spectrophotometer loaded with an integrating sphere in the visible light range of 350–800 nm at intervals of 5 nm. The contact angle (CA) measuring instrument (Kyowa Interface, Inc. Finland) was used to test the CA and sliding angle (SA) of the high transmission hydrophobic glass. The slides were leaned on the petri dish, spread a layer of 270-purpose standard quartz sand on the surface. It was used an eyedropper to absorb deionized water, which was dropped on the surface of the slides, observed the rolling of water droplets on the surface of the slides and the residual degree of quartz sand on the surface of the slides [34]. The surface transparency of the untreated slides and the coated slides were observed in contrast. The adhesion test between the film layer and the substrate was carried out in accordance with GB/T 9286-1998, Cross cut Test for Paints and Varnishes Film. A blade was used to draw 10×10 grids at 1 mm intervals on the surface of the glass substrate. The cut surface was cleaned with a soft bristled brush, and peeled off with 3 M tape to check its adhesion to the substrate [35]. In the sandpaper friction test, the 100 g weight was tightly adhered to the prepared slides coated with hydrophobic coating with glue. The coating layer contacted the surface of the sandpaper and moved in a straight line, and

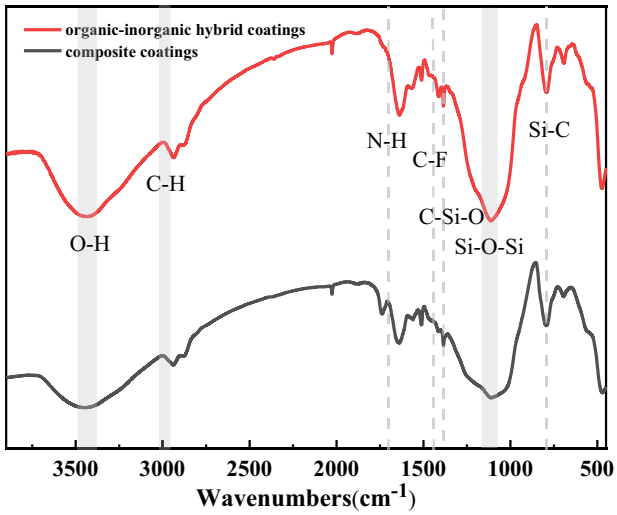

Fig. 3 The fourier transform infrared spectroscopy of organic-inorganic hybrid coating and composite coating

the contact angle of the hydrophobic coating after the above treatment was determined. An oil-based pen was used to write on the surface of bare glass and coated glass. The ink was observed on the surface of the glass, and then wiped with a tissue to observe the remaining ink on the surface of the glass. After the coated glass was soaked in pH = 2 (0.01 M HCl) and pH = 13 (0.1 M NaOH) solutions for 15 h, cleaned by ultrasound with deionized water for 20 min and dried to determine the contact angles and sliding angles of the hydrophobic coating every 3 h.

3 Results and discussion

3.1 FT-IR analysis of organic-inorganic hybrid coatings and composite coatings

The fourier transform infrared spectroscopy of composite coatings sprayed on glass surface with modified silica sol and modified with perfluoropylether based on silica sol were showed in Fig. 3. The strong absorption peak at 1100 cm^{-1} was due to stretching vibration of Si-O-Si bond. The deformation vibrations peak of C-H bond was near 2950 cm^{-1}. The wide absorption peak observed at 3400 cm^{-1} corresponded to the stretching vibration peak of O-H bond. At 3360 cm^{-1} and 1650 cm^{-1}, there were N-H stretching vibration and bending vibration peaks, respectively. The N-H stretching vibration peak might exist near 3360 cm^{-1}, but the N-H peak was covered because the O-H vibration absorption peak was too strong. The absorption peak observed at 1340 cm^{-1} represented the vibration absorption peak of C-Si-O. The peak at 760 cm^{-1} was attributed to the stretching vibration peak of Si-C bond in methylsilane [36].

Among them, the N-H bending vibration peak at 1650 cm^{-1}; the vibration absorption peaks of C-Si-O near 1390 cm^{-1}. These characteristic peaks proved that the silane coupling agent KH-550 successfully reacted with SiO_2 particles and grafted to its surface. Symmetric stretching vibration peak of C-H bond in epoxy group was around 2970 cm^{-1}; the vibration absorption peak of C-Si-O was observed at 1390 cm^{-1} and the stretching vibration peak of Si-C bond in methylsilane was found near 760 cm^{-1}. These characteristic absorption peaks proved that KH-560 was successfully grafted to the surface of SiO_2 particles.

On the basis of the organic-inorganic hybrid coating, perfluoropolyether chain was introduced into the composite coating, and the absorption peak of hydroxyl group in the composite coating was weakened, which was consistent with the theory that the hydroxyl group was consumed during the linking process of perfluoropolyether. The reduction of hydrophilic hydroxyl group also indicated that the composite coating had better hydrophobic performance, and the absorption peak of $-CF_3$ appeared at 1460 cm^{-1}. The results showed that the structure was consistent with the expected structure of composite coating and organic-inorganic hybrid coating.

3.2 Microstructure and elemental analysis of composite coatings

3.2.1 Microstructure of composite coating

The microstructures of the composite coating with different dosages of silane coupling agents were shown in Fig. 4.

It was shown that there were a large number of silica particles on the surface of the coating, and the particles were agglomerated irregularly and formed a certain roughness on the glass surface. A rough structure at the micrometer scale for the hydrophobicity of composite coatings was provided. With the increase of silane coupling agent usage, the surface roughness of the coating was increased.

3.2.2 EDS test results and analysis

The EDS spectrum and the element content of the coating were showed in Fig. 5. The contents of C, O, F and Si in the sample were 23.14%, 40.07%, 0.93% and 35.85%, respectively. The proportion of F was small, indicating that the content of perfluoropolyether chain in the composite coating was small [37].

From the analysis of the preparation mechanism of the composite coating, the linking dendrimers of perfluoropolyether was few. When the prepared silica sol was modified with KH550 and KH560, both of them were grafted by reacting with the hydroxyl group on the surface

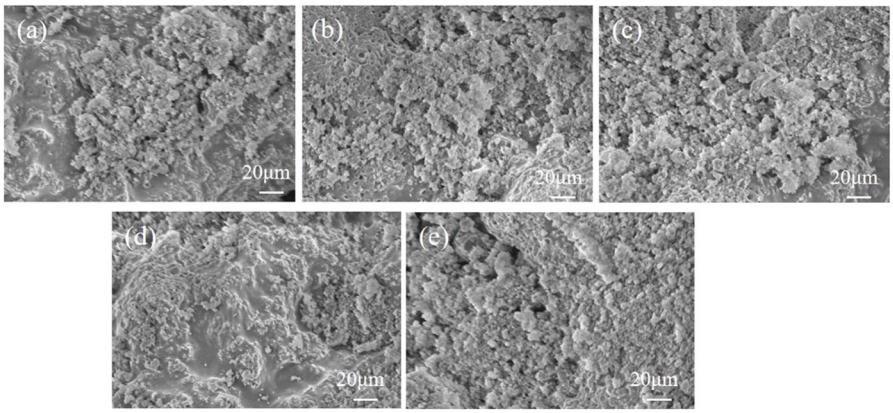

Fig. 4 Surface morphology of composite coatings prepared with different dosages of silane coupling agents. **a** 0.1%, **b** 0.2%, **c** 0.3%, **d** 0.4%, **e** 0.5%

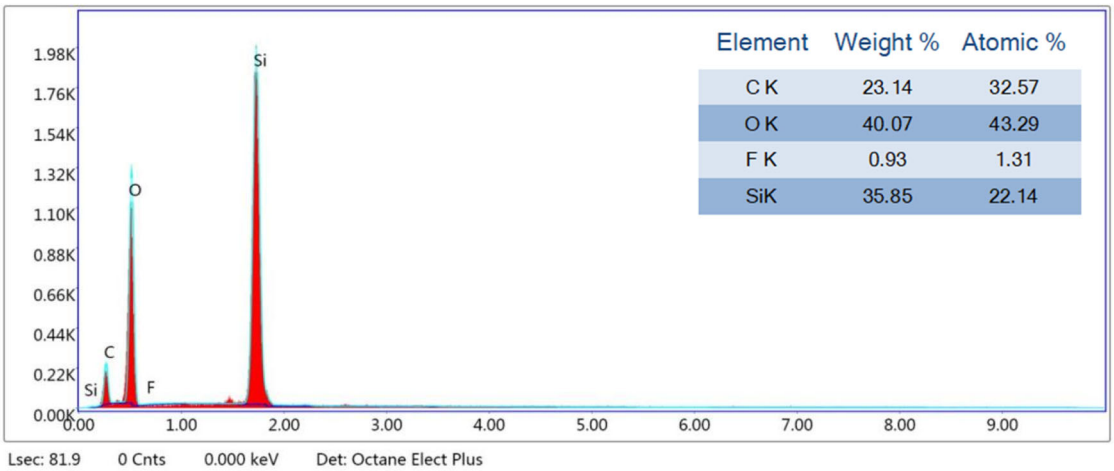

Fig. 5 EDS spectrum and content of each element

of SiO_2 microspheres. When the modified silica sol formed an organic-inorganic hybrid coating on the glass surface, the hydroxyl group on the surface of SiO_2 microspheres and the hydroxyl group on the glass surface also underwent dehydration condensation. Therefore, there were less hydroxyl groups remaining that could chemically bond with the perfluoropolyether chain, resulting in less grafting of the perfluoropolyether chain segment in the composite coating.

3.3 Effect of silane coupling agent dosage on coating transparency and hydrophobicity

3.3.1 Effect of silane coupling agent dosage on the transparency of composite coating

The hydrophobic performance of the coating was the best when the amount of KH550 and KH560 was 1:1. Therefore, this design only explored the effect of the total amount of silane coupling agent on the transparency of the composite coating. Figure 6 was filmed at night under lighting conditions, from left to right: (a) bare glass, coated glass (silane coupling agent added (b) 0.1%, (c) 0.2%, (d) 0.3%, (e) 0.4%, (f) 0.5%). As the total amount of silane coupling agent were increased, the transparency of the glass became lower and lower. When the amount of silane coupling agent was 0.1%, the transparency of coated glass was almost the same as that of bare glass. When the amount added was 0.2%, 0.3%, 0.4%, the transparency of the coated glass was decreased obviously. When the amount added was 0.5%, the transparency of the coated glass was very poor.

Figure 7 was taken under daytime lighting conditions. Consistent with the observed results in Fig. 6, the increase of the amount of silane coupling agent in the modified silica sol would reduce the transmittance of the coated glass.

The effect of silane coupling agent dosage on the transparency of the coating was shown in Fig. 8. Under UV visible near-infrared spectrophotometer testing, compared with the uncoated bare glass surface, the coating had a certain impact on the transparency of the glass. As the amount of silane coupling agent gradually increased, the transmittance of the coating in the wavelength range of 350–800 nm gradually decreased. Glass coated with 0.1% silane coupling agent had little difference in transparency compared to bare glass.

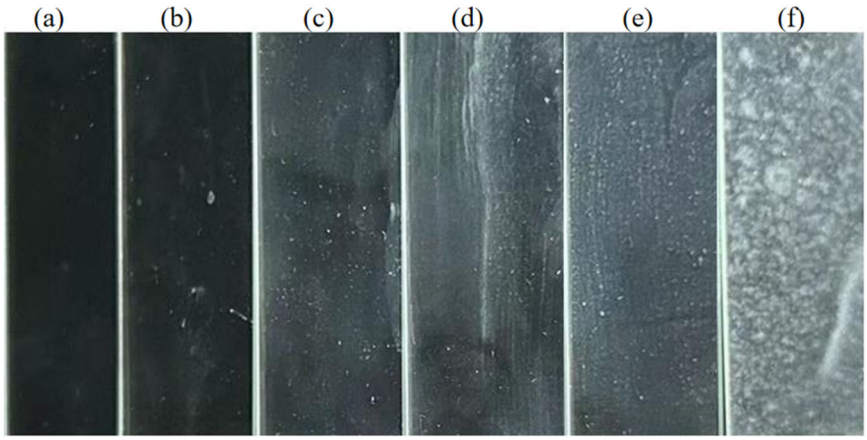

Fig. 6 Transparency of bare glass (**a**) and coated glass (night lighting condition): silane coupling agent added: **b** 0.1%, **c** 0.2%, **d** 0.3%, **e** 0.4%, **f** 0.5%

Fig. 7 Comparison of light transmittance between bare glass and coated glass (daytime lighting conditions): **a** was bare glass, and **b**–**f** were coated glasses. The dosage of silane coupling agent were (**b**) 0.1%, (**c**) 0.2%, (**d**) 0.3%, (**e**) 0.4%, and (**f**) 0.5%

3.3.2 Effect of silane coupling agent dosage on hydrophobicity of coating

The comparison of static water contact angles between bare glass and glass with an organic-inorganic hybrid coating was showed in Fig. 9. The contact angles of (a)–(f) were 33.6°, 95.3°, 108.1°, 112.8°, 113.1°, and 119.7°. It could be seen that the surface property of the bare glass was hydrophilic. With the increase of the amount of silane coupling agent, the hydrophobicity of the glass was increased. When the amount of silane coupling agent was 0.5%, the contact angle was close to 120°.

The comparison of water contact angles between bare glass and composite coated glass was showed in Fig. 10. The water contact angle of (a)–(f) were 33.6°, 103.3°, 115.1°, 124.4°, 136.0°, 140.2°. The hydrophobic properties of the glass were further improved by the composite coating on the surface of the existing rough structure. When the dosage of silane coupling agent was 0.5%, the contact angle had reached 140°. On the one hand, it was due to the reduction of hydrophilic hydroxyl group. On the other hand, it was due to the strong hydrophobicity of perfluoropolyethers with long chain and low surface energy.

Combined with the analysis of the effect of silane coupling agent on the transparency of the coating in 3.3.1, it could be seen that the experimental results were in line with the theory that transparency and roughness were competitive. The lower the transparency was, the rougher the surface structure and the better the hydrophobic property were. When the transparency requirement was high, it was more appropriate to choose 0.1% and 0.2% of silane coupling agent. When the hydrophobic performance was required, the addition amount of silane coupling agent were 0.3% or 0.4%. Although the hydrophobic performance of the glass was the best when the amount of silane coupling agent was 0.5%, its light transmittance was too low and it didn't have good application value on the glass surface. Considering the balance of transparency and hydrophobicity, the best application value could be achieved when the amount of silane coupling agent was 0.3%. The modified silane sol silane coupling agent was 0.3% in the samples prepared by a series of performance tests on the coated glass.

3.4 Adhesion performance test results and analysis

The grating knife test on the glass sprayed with composite coating used to detect the binding force between the glass surface film and the glass substrate was showed in Fig. 11. A few of the 100 grids had film layer shedding in Fig. 11a. Figure 11b was found that the film layer was obviously peeled off at the cut edge of the grid of this part. According to the test grading table, the adhesive force grade was 1~2. The adhesive force between the coating

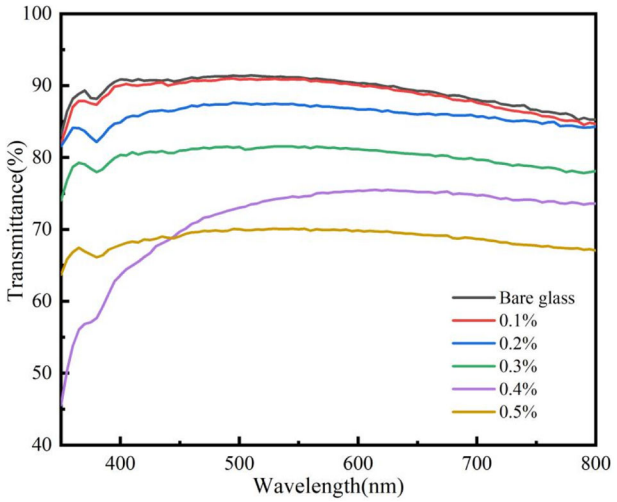

Fig. 8 Comparison chart of UV-Vis of different silane coupling agent dosages

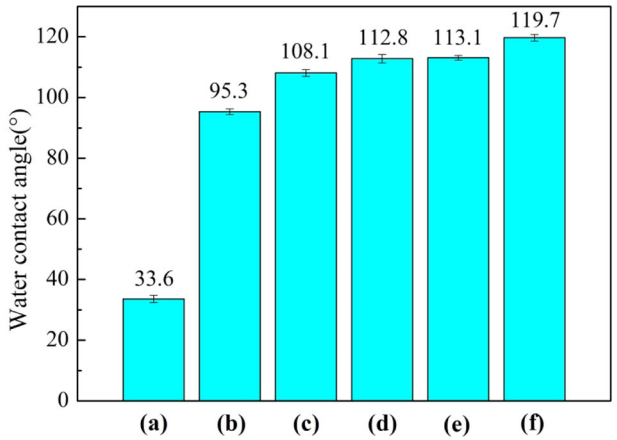

Fig. 9 Comparison of static water contact angle between bare glass and sprayed modified silica sol glass: **a** was bare glass, and the rest were coated glass, in which the dosage of silane coupling agent were successively: **b** 0.1%, **c** 0.2%, **d** 0.3%, **e** 0.4%, **f** 0.5%

and the glass substrate was good, and it had a good application prospect.

3.5 Oil pollution prevention performance test results and analysis

The oil-based pen left a continuous and uniform trace on the surface of the bare glass, and the writing effect was similar to writing on paper. However, it was difficult to write on the coated glass surface with an oil-based pen, and the ink droplets were discontinuous agglomeration in Fig. 12a. When wiping with a dry paper towel, the handwriting on the surface of the bare glass couldn't be erased, while the ink stains on the coated glass could obviously be erased in Fig. 12b.

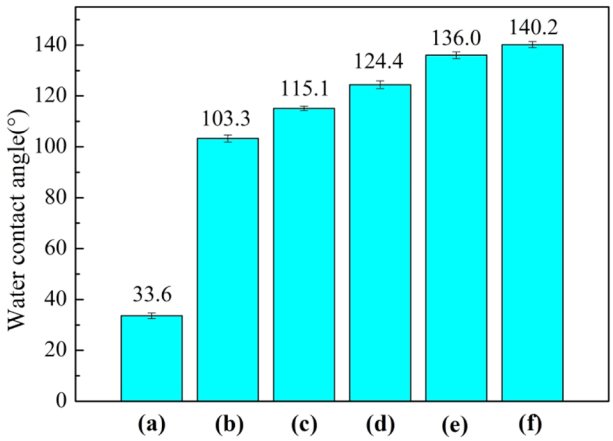

Fig. 10 Comparison of static water contact angle between bare glass and sprayed composite coated glass: **a** was bare glass, and the rest were coated glass, in which the dosage of silane coupling agent were successively: **b** 0.1%, **c** 0.2%, **d** 0.3%, **e** 0.4%, **f** 0.5%

3.6 Self-cleaning performance of the surface

After water droplets flowed down the glass surface into strands, they couldn't carry away the quartz sand. The quartz sand was still remained on the surface after completely washed in Fig. 13a–c. The quartz sand could be completely coated and took away by the water droplets without any residue on the surface in Fig. 13d–f. Figure 13g showed the SA of the composite coating.

With the increase of the proportion of silane coupling agent dosage, the SA of the composite coating was decreased. It could be seen that the coated glass had good self-cleaning performance and could be widely used in many scenarios.

3.7 Wear resistance test results and analysis

The situation of the glass surface after reciprocating friction on the coated glass was showed in Fig. 14. The reciprocating friction times were 50 times, 100 times, 300 times, and 500 times from top to bottom. The corresponding static water contact angles were 120.9°, 117.6°, 109.3°, and 96.9° respectively. When the number of reciprocating friction was 50 times, the surface film was felt off, and the contact angle was decreased from 124.4° to 120.9°. After the number of reciprocating friction reached 500 times, the film layer was felt off seriously, the contact angle was dropped to 96.9°, and there was still a certain hydrophobic property.

3.8 Acid and alkali resistance results and analysis

As shown in Fig. 15, the slide coated with composite layer was immersed in an acid or alkali solution for a total 15 h,

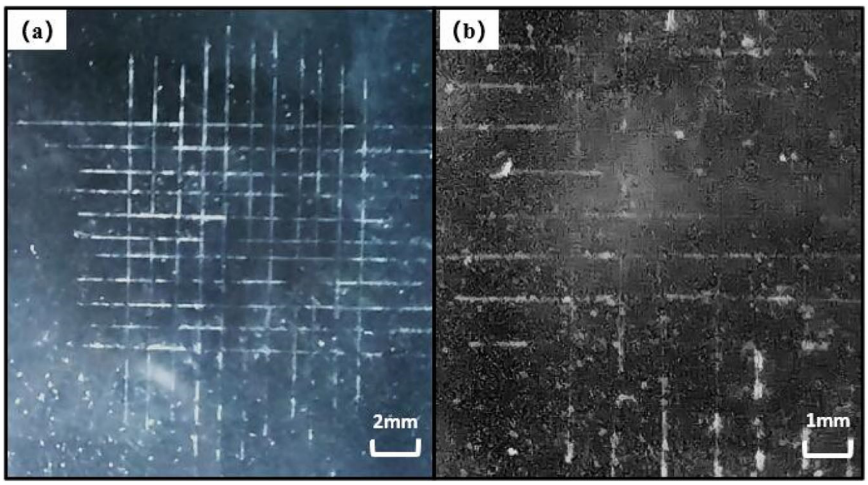

Fig. 11 Adhesion performance test: **a** the grating knife test, **b** an enlarged picture of the part of the film layer apparently falling off in the upper left corner of **a**

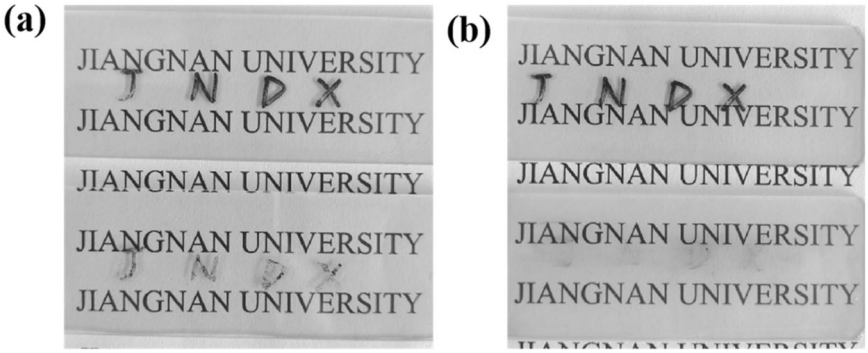

Fig. 12 Oil resistance test of bare glass and coated glass: **a** the result of writing on the surface of bare glass and coated glass with a common black marker and letting it dry for 30 s, **b** the result of wiping it with a dry paper towel for five times

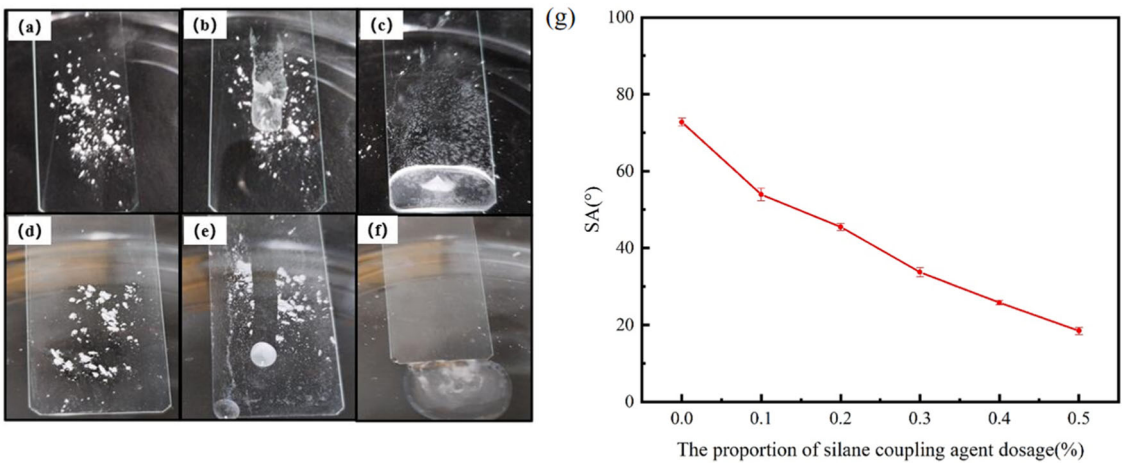

Fig. 13 Comparison of surface self-cleaning performance of bare glass and coated glass: **a**–**c** the bare glass surface, **d**–**f** the coated glass surface. **g** The SA of the composite coating

and it was taken out every 3 h, then washed with deionized water and dried. The contact and sliding angles were measured [38].

Under strong acid condition, the coating was not broken and the hydrophobicity was almost unchanged. However, the hydrophobic property of the coated glass was greatly reduced when the coating was destroyed under strong alkaline conditions. It was concluded that the composite coating was resistant to strong acid but not strong alkali.

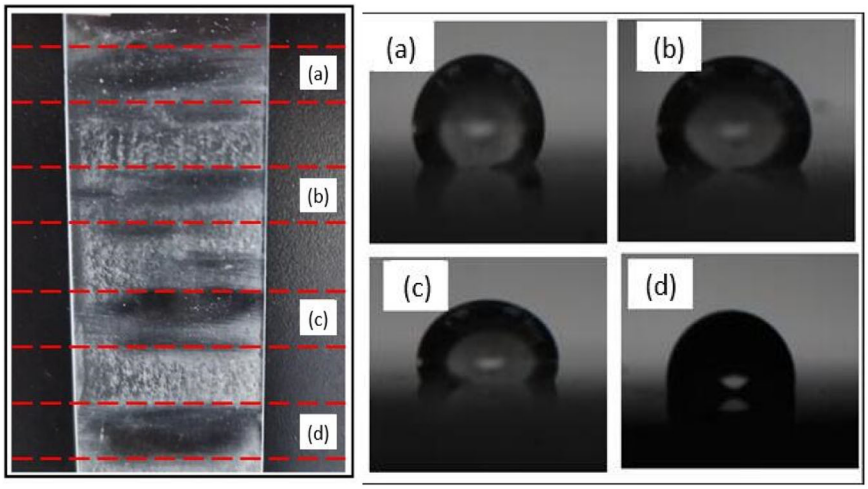

Fig. 14 Friction resistance test of coated glass and corresponding water contact angle: **a** 50 times, **b** 100 times, **c** 300 times, **d** 500 times

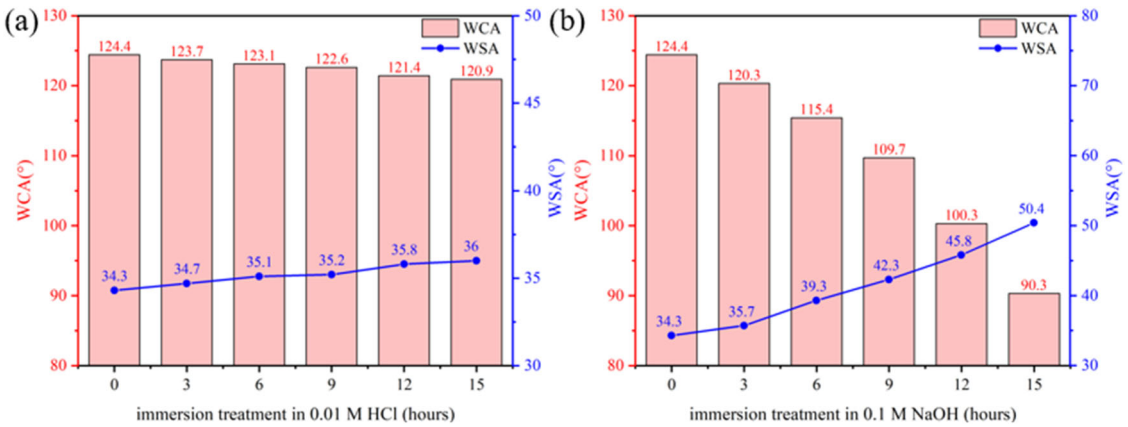

Fig. 15 The water contact and sliding angles of composite coatings after immersion treatment in (**a**) 0.01 M HCl and (**b**) 0.1 M NaOH solutions for 15 h

4 Conclusions

In this paper, the silica sol was prepared by sol-gel method. Then the silica sol was functionally modified by silane coupling agent, and water-based silicone resin was added to obtain the modified silica sol with good dispersion and stability. After spraying on the glass surface, an organic-inorganic nanocomposite rough structure was constructed. Further spraying of nano-fluorocarbon polymer was equivalent to using low surface energy material perfluoropolyl polymer for surface modification, and then spraying on the glass to obtain a chemically bonded composite coating. The increase in the amount of silane coupling agent led to a decrease in the transparency of the coating when the amount of silane coupling agent was 0.1%, the transparency of coated glass was almost the same as that of bare glass. When the amounts were 0.2%, 0.3%, 0.4%, the transparency of the coated glass decreased obviously. When the amount was 0.5%, the transparency of the coated glass was very poor. The test results showed that the coating had good adhesion, good self-cleaning effect, wear resistance, acid resistance but poor alkali resistance.

Acknowledgements This work is supported by the Project funded by China Postdoctoral Science Foundation (2023M743127), Nantong Basic Science Research Program (JCZ2022100, JC2023068), Science and Technology Guiding program of China Textile Industry Federation (2022032), Qing Lan Project of Jiangsu University and Opening Project of Hubei Key Laboratory of Biomass Fibers & Eco-Dyeing & Finishing (Wuhan Textile University) (STRZ202312).

Author contributions JL: conceptualization, methodology, writing-original draft, writing-review and editing. QK: investigation, formal analysis, validation. DZ: supervision, writing-review and editing, funding acquisition. ZL: investigation, formal analysis, data curation.

Compliance with ethical standards

Conflict of interest The authors declare no competing interests.

References

1. Xie Z, Wang H, Geng Y, Li M, Deng Q, Tian Y, Chen R, Zhu X, Liao Q (2021) Carbon-based photothermal superhydrophobic materials with hierarchical structure enhances the anti-Icing and photothermal deicing properties. ACS Appl Mater Interfaces 13(40):48308–48321. https://doi.org/10.1021/acsami.1c15028
2. Park C, Kim T, Kim Y-I, Lee MW, An S, Yoon SS (2021) Supersonically sprayed transparent flexible multifunctional composites for self-cleaning, anti-icing, anti-fogging, and antibacterial applications. Compos Part B Eng 222:109070. https://doi.org/10.1016/j.compositesb.2021.109070
3. Liu X, Chen H, Zhao Z, Zhu Y, Wang Z, Chen J, Zhang D (2021) Tunable self-jumping of melting frost on macro-patterned anisotropic superhydrophobic surfaces. Surf Coat Technol 409:126858. https://doi.org/10.1016/j.surfcoat.2021.126858
4. Chen G, Wang Y, Qiu J, Cao J, Zou Y, Wang S, Ouyang J, Jia D, Zhou Y (2021) A visibly transparent radiative cooling film with self-cleaning function produced by solution processing. J Mater Sci Technol 90:76–84. https://doi.org/10.1016/j.jmst.2021.01.092
5. Li W, Zhang Y, Yu Z, Zhu T, Kang J, Liu K, Li Z, Tan SC (2022) In situ growth of a stable metal–organic framework (MOF) on flexible fabric via a layer-by-layer strategy for versatile applications. ACS Nano 16(9):14779–14791. https://doi.org/10.1021/acsnano.2c05624
6. Jin K, Zhang M, Wang J, Jin Z, Sun J, Zhao Y, Xie K, Cai Z (2022) Robust highly conductive fabric with fluorine-free healable superhydrophobicity for the efficient deicing of outdoor's equipment. Colloids Surf A Physicochemical Eng Asp 651:129639. https://doi.org/10.1016/j.colsurfa.2022.129639
7. Ng Y-H, Tay SW, Hong L (2022) Ice-phobic polyurethane composite coating characterized by surface micro silicone loops with crumpling edges. Prog Org Coat 172:107058. https://doi.org/10.1016/j.porgcoat.2022.107058
8. Krishnan A, Krishnan AV, Ajith A, Shibli SMA (2021) Influence of materials and fabrication strategies in tailoring the anticorrosive property of superhydrophobic coatings. Surf Interfaces 25:101238. https://doi.org/10.1016/j.surfin.2021.101238
9. Al-Qahtani SD, Al-nami SY, Alkhamis K, Al-Ahmed ZA, Binyaseen AM, Khalifa ME, El-Metwaly NM (2022) Simple preparation of long-persistent luminescent paint with superhydrophobic anticorrosion efficiency from cellulose nanocrystals and an acrylic emulsion. Ceram Int 48(5):6363–6371. https://doi.org/10.1016/j.ceramint.2021.11.179
10. Ahmed MMM, Chi Y-T, Hung Y-H, Reyes LMC, Yeh J-M (2022) UV-cured electroactive polyurethane acrylate coatings with superhydrophobic surface structure of biomimetic peacock feather for anticorrosion application. Prog Org Coat 165:106679. https://doi.org/10.1016/j.porgcoat.2021.106679
11. Luo J, Gao S, Luo H, Wang L, Huang X, Guo Z, Lai X, Lin L, Li RKY, Gao J (2021) Superhydrophobic and breathable smart MXene-based textile for multifunctional wearable sensing electronics. Chem Eng J 406:126898. https://doi.org/10.1016/j.cej.2020.126898
12. Li W, Xi Y, Li Z (2021) Anisotropic overgrowth of metal heterostructures regulated by a hydrophobic grafting layer towards self-cleaning and oil/water separation applications. Surf Coat Technol 427:127814. https://doi.org/10.1016/j.surfcoat.2021.127814
13. Li W, Liu K, Zhang Y, Guo S, Li Z, Tan SC (2022) A facile strategy to prepare robust self-healable superhydrophobic fabrics with self-cleaning, anti-icing, UV resistance, and antibacterial properties. Chem Eng J 446:137195. https://doi.org/10.1016/j.cej.2022.137195
14. Dong X, Gao S, Huang J, Li S, Zhu T, Cheng Y, Zhao Y, Chen Z, Lai Y (2019) A self-roughened and biodegradable superhydrophobic coating with UV shielding, solar-induced self-healing and versatile oil–water separation ability. J Mater Chem A 7(5):2122–2128. https://doi.org/10.1039/C8TA10869B
15. Kaldellis JK, Kapsali M (2011) Simulating the dust effect on the energy performance of photovoltaic generators based on experimental measurements. Energy 36(8):5154–5161. https://doi.org/10.1016/j.energy.2011.06.018
16. Sulaiman SA, Singh AK, Mokhtar MMM, Bou-Rabee MA (2014) Influence of Dirt Accumulation on Performance of PV Panels. Energy Procedia 50:50–56. https://doi.org/10.1016/j.egypro.2014.06.006
17. Barthlott W, Neinhuis C (1997) Purity of the sacred lotus, or escape from contamination in biological surfaces. Planta 202(1):1–8. https://doi.org/10.1007/s004250050096
18. Xu Y, Fan WH, Li ZH, Wu D, Sun YH (2003) Antireflective silica thin films with super water repellence via a solgel process. Appl Opt 42(1):108–112. https://doi.org/10.1364/AO.42.000108
19. Nakajima A, Fujishima A, Hashimoto K, Watanabe T(1999) Preparation of transparent superhydrophobic boehmite and silica films by sublimation of aluminum acetylacetonate Adv Mater 11(16):1365–1368. https://doi.org/10.1002/(SICI)1521-4095(199911)11:16<1365::AID-ADMA1365>3.3.CO;2-6
20. Tian J, Bao J, Li L, Sha J, Duan W, Qiao M, Cui J, Zhang Z (2023) Facile fabrication of superhydrophobic coatings with superior corrosion resistance on LA103Z alloy by one-step electrochemical synthesis. Surf Coat Technol 452:129090. https://doi.org/10.1016/j.surfcoat.2022.129090
21. Liu H, Gao SW, He JS, Mao CL, Jun J (2016) Recent progress in fabrication and applications of superhydrophobic coating on cellulose-based substrates. Mater Des 9(3):124. https://doi.org/10.3390/ma9030124
22. Khan MZ, Baheti V, Militky J, Ali A, Vikova M (2018) Superhydrophobicity, UV protection and oil/water separation properties of fly ash/Trimethoxy(octadecyl)silane coated cotton fabrics. Carbohydr Polym 202:571–580. https://doi.org/10.1016/j.carbpol.2018.08.145
23. Wang H, Zhang Y, Xue F, Bai W, Shi X, Liu Y, Feng L (2021) One-step environment-friendly process to design fire-resistant superhydrophobic carbon felts with excellent durability and oil–water separation performance. J Mater Sci 56(21):12183–12197. https://doi.org/10.1007/s10853-021-06076-w
24. Zhang Y, Ge D, Yang S (2014) Spray-coating of superhydrophobic aluminum alloys with enhanced mechanical robustness. J Colloid Interface Sci 423:101–107. https://doi.org/10.1016/j.jcis.2014.02.024
25. Aminayi P, Abidi N (2013) Imparting super hydro/oleophobic properties to cotton fabric by means of molecular and nanoparticles vapor deposition methods. Appl Surf Sci 287:223–231. https://doi.org/10.1016/j.apsusc.2013.09.132
26. Lin D, Zeng X, Li H, Lai X, Wu T (2019) One-pot fabrication of superhydrophobic and flame-retardant coatings on cotton fabrics via sol-gel reaction. J Colloid Interface Sci 533:198–206. https://doi.org/10.1016/j.jcis.2018.08.060
27. Bake A, Merah N, Matin A, Gondal M, Qahtan T, Abu-Dheir N (2018) Preparation of transparent and robust superhydrophobic surfaces for self-cleaning applications. Prog Org Coat 122:170–179. https://doi.org/10.1016/j.porgcoat.2018.05.018
28. Gore PM, Kandasubramanian B (2018) Heterogeneous wettable cotton based superhydrophobic Janus biofabric engineered with PLA/functionalized-organoclay microfibers for efficient oil-water separation. J Mater Chem A 6(17):7457–7479. https://doi.org/10.1039/c7ta11260b
29. Liu Z, Wang H, Zhang X, Wang C, Lv C, Zhu Y (2017) Durable and self-healing superhydrophobic surface with bistratal gas layers

prepared by electrospinning and hydrothermal processes. Chem Eng J 326:578–586. https://doi.org/10.1016/j.cej.2017.05.142
30. Zhang F, Shi Z, Jiang Y, Xu C, Wu Z, Wang Y, Peng C (2017) Fabrication of transparent superhydrophobic glass with fibered-silica network. Appl Surf Sci 407:526–531. https://doi.org/10.1016/j.apsusc.2017.02.207
31. Gao Y, Li Z, Cheng B, Su K (2018) Superhydrophilic poly(p-phenylene sulfide) membrane preparation with acid/alkali solution resistance and its usage in oil/water separation. Sep Purif Technol 192:262–270. https://doi.org/10.1016/j.seppur.2017.09.065
32. Cai A, Yan X, Ye X (2020) Preparation and characterization of polyurethane-SiO_2 composite super-hydrophilic transparent coating with self-cleaning and anti-fog. Acta Mater Compositae Sin 37(01):191–197. https://doi.org/10.13801/j.cnki.fhclxb.20190505.004
33. Sun X, Li L, Xu X, Song G, Tu J, Yan P, Zhang W, Hu K (2020) Preparation of hydrophobic SiO_2/PTFE sol and antireflective coatings for solar glass cover. Optik 212:164704. https://doi.org/10.1016/j.ijleo.2020.164704
34. Luo M, Sun X, Zheng Y, Cui X, Ma W, Han S, Zhou L, Wei X (2023) Non-fluorinated superhydrophobic film with high transparency for photovoltaic glass covers. Appl Surf Sci 609:155299. https://doi.org/10.1016/j.apsusc.2022.155299
35. Lei Y, Jiang B, Liu H, Zhang F, An Y, Zhang Y, Yuan Y, Xu J, Li X, Liu T (2023) Mechanically robust superhydrophobic polyurethane coating for anti-icing application. Prog Org Coat 183:107795. https://doi.org/10.1016/j.porgcoat.2023.107795
36. Liao G, Yao W, She A, Bian X (2023) An eco-friendly building coating with high self-cleaning capacity: Synergetic effect of super-hydrophobicity and photocatalytic degradation. Constr Build Mater 406:133406. https://doi.org/10.1016/j.conbuildmat.2023.133406
37. He Q, Wang J, Wang G, Hao X, Li A (2023) Construction of a durable superhydrophobic flame-retardant coating on the PET fabrics. Mater Des 233:112258. https://doi.org/10.1016/j.matdes.2023.112258
38. Choi Y-J, Ko JH, Jin S-W, Jin Y-J, Park C-H, Jang Y-J, Chung C-M (2024) Transparent, superhydrophobic, and flexible polyimide films with robust and durable imide/silica particles surface prepared via a sintering process. Surf Interfaces 46:104099. https://doi.org/10.1016/j.surfin.2024.104099